

**This is a self-archived version of an original article. This version may differ from the original in pagination and typographic details.**

**Author(s):** Auranen, K.; Jakobsson, U.; Badran, H.; Grahn, T.; Greenlees, P. T.; Herzán, A.; Julin, R.; Juutinen, S.; Konki, J.; Leino, M.; Leppänen, A.-P.; O'Neill, G.; Pakarinen, J.; Papadakis, P.; Partanen, J.; Rahkila, P.; Ruotsalainen, P.; Sandzelius, M.; Sarén, J.; Scholey, C.; Sinclair, L.; Sorri, J.; Stolze, S.; Uusitalo, J.; Voss, A.

**Title:** Isomeric  $13/2^+$  state in  $201\text{Fr}$

**Year:** 2020

**Version:** Published version

**Copyright:** ©2020 American Physical Society

**Rights:** In Copyright

**Rights url:** <http://rightsstatements.org/page/InC/1.0/?language=en>

**Please cite the original version:**

Auranen, K., Jakobsson, U., Badran, H., Grahn, T., Greenlees, P. T., Herzán, A., Julin, R., Juutinen, S., Konki, J., Leino, M., Leppänen, A.-P., O'Neill, G., Pakarinen, J., Papadakis, P., Partanen, J., Rahkila, P., Ruotsalainen, P., Sandzelius, M., Sarén, J., . . . Voss, A. (2020). Isomeric  $13/2^+$  state in  $201\text{Fr}$ . *Physical Review C*, 101(2), Article 024306. <https://doi.org/10.1103/PhysRevC.101.024306>

Isomeric  $13/2^+$  state in  $^{201}\text{Fr}$ 

K. Auranen<sup>1,\*</sup>, U. Jakobsson,<sup>1</sup> H. Badran,<sup>1</sup> T. Grahn,<sup>1</sup> P. T. Greenlees,<sup>1</sup> A. Herzáň,<sup>1,2</sup> R. Julin,<sup>1</sup> S. Juutinen,<sup>1</sup> J. Konki,<sup>1,†</sup> M. Leino,<sup>1</sup> A.-P. Leppänen,<sup>3</sup> G. O'Neill,<sup>1,4</sup> J. Pakarinen,<sup>1</sup> P. Papadakis,<sup>1,‡</sup> J. Partanen,<sup>1,§</sup> P. Rahkila,<sup>1</sup> P. Ruotsalainen,<sup>1</sup> M. Sandzelius,<sup>1</sup> J. Sarén,<sup>1</sup> C. Scholey,<sup>1,||</sup> L. Sinclair,<sup>1,5</sup> J. Sorri,<sup>1,¶</sup> S. Stolze,<sup>1,\*\*</sup> J. Uusitalo,<sup>1</sup> and A. Voss<sup>1</sup>

<sup>1</sup>University of Jyväskylä, Department of Physics, P.O. Box 35, FI-40014 University of Jyväskylä, Finland

<sup>2</sup>Institute of Physics, Slovak Academy of Sciences, SK-84511 Bratislava, Slovakia

<sup>3</sup>Radiation and Nuclear Safety Authority–STUK, Lähteentie 2, 96400, Rovaniemi, Finland

<sup>4</sup>University of Liverpool, Department of Physics, Oliver Lodge Laboratory, Liverpool L69 7ZE, United Kingdom

<sup>5</sup>Department of Physics, University of York, Heslington, York, YO10 5DD, United Kingdom



(Received 19 December 2019; accepted 30 January 2020; published 18 February 2020)

We have identified an isomeric state in  $^{201}\text{Fr}$  for which we propose a spin and parity of  $13/2^+$ , and interpret it as arising from the  $\pi(i_{13/2})$  configuration. A half-life of 720(40) ns was measured, corresponding to  $B(M2) = 0.17(2)$  W.u., in good agreement with those of other  $13/2^+ \rightarrow 9/2^- [\pi(i_{13/2}) \rightarrow \pi(h_{9/2})]$  transitions observed in other nuclei in the region. The nuclei of interest were produced in a fusion-evaporation reaction and their decay properties were investigated using the GREAT spectrometer at the focal plane of the RITU gas-filled recoil separator.

DOI: [10.1103/PhysRevC.101.024306](https://doi.org/10.1103/PhysRevC.101.024306)

## I. INTRODUCTION

One of the typical properties of nuclei in the region beyond lead is the presence of various isomeric states [1]. In the odd-mass nuclei a low-spin isomeric intruder  $1/2^+$  state, interpreted to arise from a  $\pi(s_{1/2}^{-1})$  configuration, has been observed in bismuth (see Ref. [2] and references therein), astatine [3–7], and francium nuclei [8–12]. The energy of this state decreases with decreasing neutron number along an isotopic chain, providing an experimental signature of the onset of oblate deformation and increasing collectivity. The  $1/2^+$  state becomes the ground state at  $^{185}\text{Bi}$  [2] and  $^{195}\text{At}$  [5], and it might become the ground state of francium starting at  $^{199}\text{Fr}$  [8,11,12]. In this publication we report an improved half-life value for the  $\alpha$ -decaying  $1/2^+$  isomeric state in  $^{201}\text{Fr}$ . The present data remove the issue of anomalously large reduced  $\alpha$ -decay widths reported in Refs. [8,13], which were obtained with very limited statistics.

The primary purpose of this work, however, is to expand the knowledge on the isomeric  $13/2^+ [\pi(i_{13/2})]$  state. Similar to

the  $1/2^+$  state, the  $13/2^+$  state is well known throughout the bismuth and astatine isotopes and has been associated with oblate deformation (see, for example, Refs. [2,14–16] and references therein). In the astatine isotopes, consistent with the oblate deformed interpretation, a rotational band has been identified above the  $13/2^+$  state in the  $^{199,197,195}\text{At}$  isotopes [17,18]. In francium isotopes, the state has been characterized in  $^{205}\text{Fr}$  [10] and  $^{203}\text{Fr}$  [9], the former having a similar rotational band built on the  $13/2^+$  state, whereas a tentative assignment for the beginning of said band has been made for the latter. In Ref. [13] an isomeric state with  $T_{1/2} = 700_{-200}^{+500}$  ns was reported in  $^{201}\text{Fr}$ . Based on Weisskopf estimates, an  $M2$  transition was proposed to depopulate this isomer. A level energy of 101–300 keV was estimated based on  $K$ -shell atomic electron binding energy and the trends of the internal-conversion coefficient  $\alpha_K$  for an  $M2$ -type transition as a function of transition energy. In this work we provide improved experimental evidence for the level energy and half-life of the isomer, as well as for the  $M2$  character of the depopulating transition. The obtained results are compared to the systematics of  $13/2^+$  states observed in the region.

## II. EXPERIMENTAL DETAILS

The experiment was carried out at the Accelerator Laboratory of the University of Jyväskylä. The nuclei of interest were produced in the fusion-evaporation reaction  $^{169}\text{Tm}(^{36}\text{Ar}, 4n)^{201}\text{Fr}$ . The experimental details used at different phases of this study are listed in Table I, and the results reported here represent the sum of all the data. The fusion-evaporation residues recoiling out of the target (referred as recoils hereafter) were filtered from the primary beam using the RITU separator [19,20] and subsequently studied at the

\*kalle.e.k.auranen@jyu.fi

†Present address: CERN, CH-1211, Geneva 23, Switzerland.

‡Present address: STFC Daresbury Laboratory, Daresbury, Warrington WA4 4AD, United Kingdom.

§Deceased.

||Present address: MTC Limited, Ansty Park, Coventry CV79JU, United Kingdom.

¶Present address: Radiation and Nuclear Safety Authority–STUK, Laippatie 4, 00880 Helsinki, Finland.

\*\*Present address: Physics Division, Argonne National Laboratory, 9700 South Cass Avenue, Lemont, IL 60439, USA.

TABLE I. The beam energies ( $E_b^{\text{LAB}}$ ), the typical beam intensities ( $I_b$ ), the irradiation times ( $t$ ), and the thicknesses of the thulium target ( $d_{\text{Tm}}$ ) and possible  $^{12}\text{C}$  degrader foils ( $d_C^U$  and  $d_C^D$ , stacked upstream and downstream of the target, respectively) used at different phases of this study.

Phase	$E_b^{\text{LAB}}$ (MeV)	$I_b$ (pnA)	$t$ (h)	$d_{\text{Tm}}$ ( $\mu\text{g}/\text{cm}^2$ )	$d_C^U$ ( $\mu\text{g}/\text{cm}^2$ )	$d_C^D$ ( $\mu\text{g}/\text{cm}^2$ )
1	178	90	8	1000	0	70
2	184	100	6	1000	0	70
3	187	120	38	1000	177	0
4	187	75	1	410	200	70
5	187	100	49	1000	200	70

focal plane of the RITU using the GREAT spectrometer [21]. The recoils passed through a multiwire proportional counter (MWPC), after which they were implanted into a 300- $\mu\text{m}$ -thick double-sided silicon strip detector (DSSD). The high-granularity DSSD was used to correlate spatially the recoils, identified based on their energy loss in the MWPC and on the MWPC-DSSD time-of-flight, with the subsequent  $\alpha$ -decay events. An event without the MWPC signal was considered as a decay event. Known as the recoil-decay tagging, the above-described method is extremely selective and therefore suitable for the studies of the weakest production channels. A cross section of the order of 6 nb was estimated for the production of  $^{201}\text{Fr}$  based on the number of observed  $\alpha$ -decay events. An array of silicon PIN diodes was assembled in a tunnel geometry upstream from the DSSD. The PIN diodes were used to detect internal-conversion electrons and  $\alpha$  particles escaping from the DSSD. Delayed  $\gamma$  rays were detected using three clover-type germanium detectors outside the GREAT vacuum chamber and one planar-type detector placed immediately behind the DSSD, inside the vacuum space. Data from all detectors were time stamped with a 100-MHz clock, and the GRAIN software package [22] was employed in the analysis.

### III. RESULTS AND DISCUSSION

The events of interest were identified by searching for recoil-implantation events, subsequently correlated with an  $\alpha$ -decay event of  $^{201}\text{Fr}$  in the same pixel of the DSSD. The efficiency of the setup was enhanced further by adding back the energies of the escaped  $\alpha$  particles observed in the PIN diodes. An energy spectrum of internal conversion electrons, observed in the PIN diodes within 5  $\mu\text{s}$  of the preceding recoil implantation, is displayed in Fig. 1(a). The two peaks of the spectrum fit to the energies of a  $K$  and  $L + M + \dots$  internal conversion of a 289.5-keV transition. A  $K/L+M+\dots$  intensity ratio of 3.0(9) was extracted, in good agreement with a theoretical value of 2.7(3) obtained for a 289.5-keV  $M2$ -type transition using the BrIcc calculator [24]. The transition energy of 289.5(4) keV was obtained by fitting the  $\gamma$ -ray energy spectrum displayed in Fig. 1(b), in which the data from the clover- and planar-type detectors were combined under the same conditions as for the electrons of Fig 1(a).

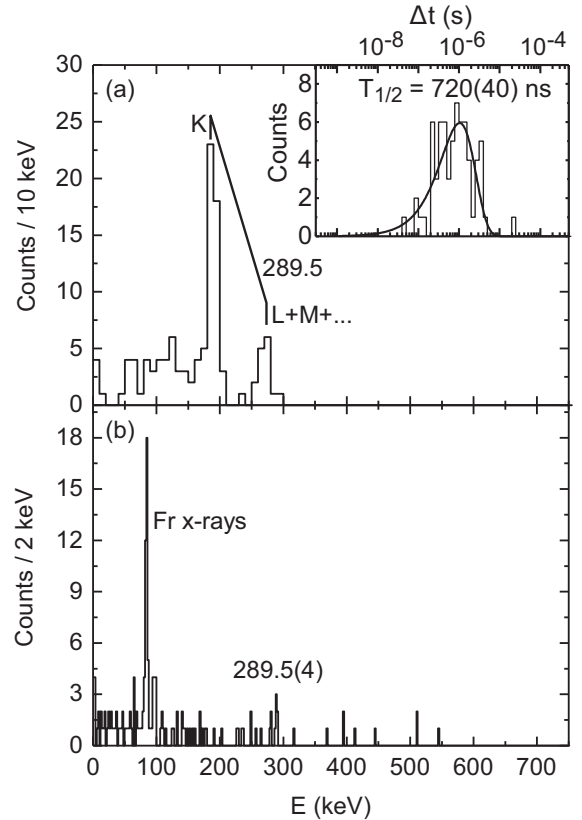


FIG. 1. (a) Energy spectrum of internal conversion electrons emitted in the decay of the  $^{13/2^+}$  isomeric state in  $^{201}\text{Fr}$ . The decay-time distribution of the electrons is displayed in the inset, and the solid line is a least-square fit [23] to the data. (b) The respective  $\gamma$ -ray energy spectrum. See the text for details.

As the  $\alpha$  decay of the  $^{201}\text{Fr}$  ground state into the  $(9/2^-)$  ground state of  $^{197}\text{At}$  exhibits allowed character [8,13], indicating a  $(9/2^-)$  ground state for  $^{201}\text{Fr}$ , we assign a spin and parity of  $(^{13/2^+})$  for the presently observed isomeric state deexcited by the  $M2$  transition to the  $^{201}\text{Fr}$  ground state. A comparison of the deduced level energy to those of the nearby  $^{13/2^+}$  ( $\pi i_{13/2}$ ) states is presented in Fig. 2(a). The level energy is seen to reduce with increasing proton number as the Fermi surface comes closer to the  $\pi i_{13/2}$  orbital as the proton levels are filled. In bismuth nuclei the  $^{13/2^+}$  level energy appears to be stable near the  $N = 126$  shell closure, and then it plateaus again near the  $N = 104$  neutron-midshell, in between having a well-pronounced transitional region of 3–4 odd-mass isotopes where the energy of the state drops over 1 MeV. In astatine nuclei a similar trend has been observed, yet the transitional region is not as pronounced as in bismuth nuclei. The present level energy indicates an even more gradual decrease in the francium isotopes. This can be expected when one moves towards heavier elements, away from the  $Z = 82$  shell closure due to earlier onset of deformation. The downsloping trend of the  $^{13/2^+}$  level energy as a function of decreasing neutron number is interpreted as a fingerprint of the onset of deformation and is illustrated in Fig 3. In this figure the  $^{13/2^+}$  state excitation energy is

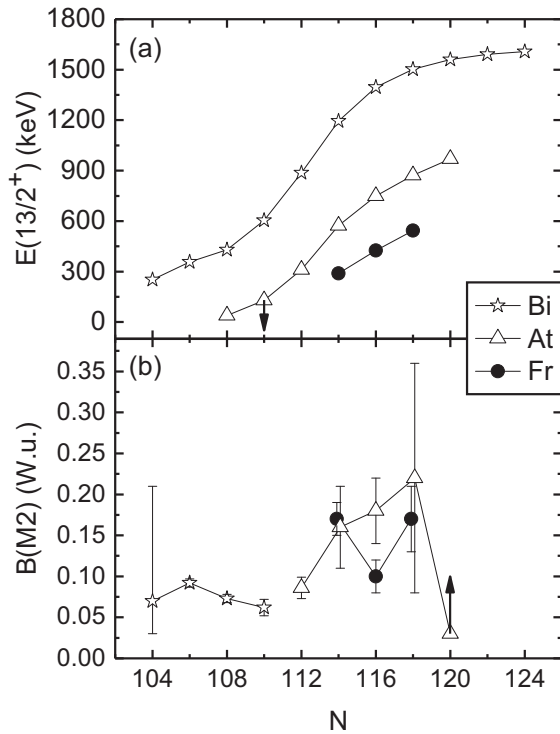


FIG. 2. (a) Level energy of the  $13/2^+$  ( $\pi i_{13/2}$ ) state in bismuth, astatine, and francium isotopes. (b) The reduced transition strength of the  $M2$  transition depopulating the  $13/2^+$  state. The neutron number of  $^{201}\text{Fr}$  is 114. Two of the data points are upper (lower) limits as indicated with the downward (upward) arrow. Some of the data points in panel (b) are slightly shifted horizontally for better visualization. Data for bismuth isotopes were obtained from Refs. [14,25–32], for astatine from Refs. [4,15–18,33–35], and for francium nuclei from this work and Refs. [9,10].

plotted against the ground-state deformation obtained from the laser spectroscopy studies. From Fig. 3 it is evident that there is a striking, seemingly linear correlation between the level energy and the ground-state deformation. This correlation can be understood through the Nilsson model, in which the  $13/2^+[606]$  proton orbital of  $\pi i_{13/2}$  spherical parentage approaches the Fermi surface in an essentially linear manner as the nucleus takes on oblate deformation. Should a similar trend occur also in francium isotopes, a ground-state deformation of  $\approx 0.15$  in magnitude can be reasonably expected for  $^{201}\text{Fr}$  (see the dashed line in Fig. 3). This is in reasonable agreement with the value of  $\approx 0.14$  predicted by the Hartree-Fock-Bogoliubov calculations [36] based on the D1S Gogny effective nucleon-nucleon interaction, but contradicts the value of  $-0.217$  predicted through the finite-range droplet model [37].

The decay-time distribution of the electrons of Fig. 1(a) is displayed in the inset, and a half-life of 720(40) ns was obtained through the least-square fitting method described in Ref. [23]. This half-life yields a reduced transition strength of 0.17(2) W.u., in agreement with those of other  $M2$  ( $\pi i_{13/2} \rightarrow \pi h_{9/2}$ ) transitions observed in nearby nuclei [see Fig. 2(b) for

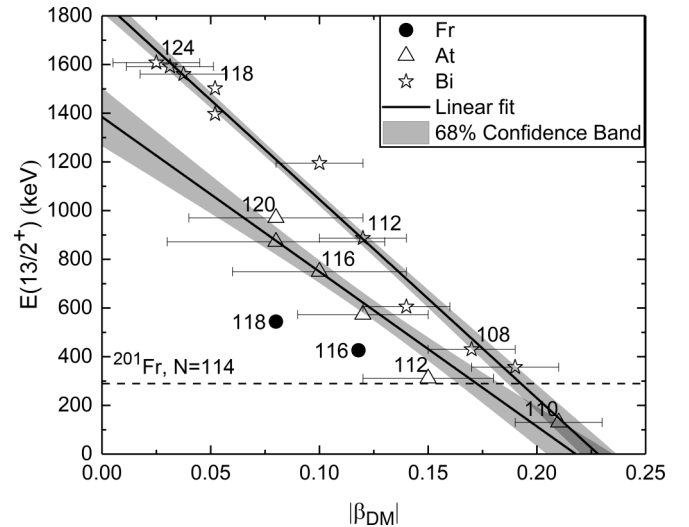


FIG. 3. The energy of the  $13/2^+$  state as a function of the magnitude of the ground-state deformation. The solid lines are a linear fit to the bismuth and astatine data, intended to guide the eye. The level energy of  $^{201}\text{Fr}$  ( $N = 114$ ) obtained in the present work is marked with a dashed line, and the numbers adjacent to some of the data points denote the neutron number of the given nucleus. The level-energy data was obtained from the references listed in the caption of Fig. 2, whereas the droplet model deformation ( $|\beta_{DM}|$ ) is that obtained through laser spectroscopy studies [38–42]. The deformation of  $^{199,201}\text{Bi}$  ( $N = 116$  and  $118$ ) isotopes is experimentally unknown; for completeness, a quadrupole deformation predicted by the finite-range droplet model [37] is used.

comparison]. This further supports the ( $13/2^+$ )  $\pi i_{13/2}$  assignment for the observed isomeric state in  $^{201}\text{Fr}$ .

As a separate observation, the half-life of the  $\alpha$ -decaying  $1/2^+ \pi(s_{1/2}^{-1})$  isomeric state in  $^{201}\text{Fr}$  was improved due to the higher level of statistics obtained. This state has been identified in Refs. [8,13], both reporting three correlated decay events. In the present study altogether 14 correlated  $^{201}\text{Fr}(1/2^+) \rightarrow ^{197}\text{At}(1/2^+) \rightarrow ^{193}\text{Bi}(1/2^+) \alpha$ -decay chains were observed. A comparison of the present results to those reported earlier is presented in Table II. Within the uncertainties, the present half-life is in agreement with that of Ref. [8], but is in contrast to that of Ref. [13]. In Ref. [8] it was speculated that the large reduced  $\alpha$ -decay width of  $^{201}\text{Fr}(1/2^+)$  might be due to an  $E3$  transition competing with the  $\alpha$  decay. The

TABLE II. Decay properties of the  $\alpha$ -emitting isomeric  $1/2^+ \pi(s_{1/2}^{-1})$  state in  $^{201}\text{Fr}$ . Reduced  $\alpha$ -decay widths ( $\delta_\alpha^2$ ) were calculated with the method described by Rasmussen [43] assuming  $\alpha$ -particle emission with  $l = 0$  and a 100%  $\alpha$ -decay branch.  $N$  is the number of observed  $\alpha$ -decay events in a given study.

Ref.	$E_\alpha$ (keV)	$T_{1/2}$ (ms)	$\delta_\alpha^2$ (keV)	$N$
This work	7457(9)	$37_{-8}^{+14}$	$64_{-21}^{+24}$	14
[8]	7454(8)	$19_{-6}^{+19}$	126(71)	3
[13]	7445(8)	$8_{-3}^{+12}$	$300_{-100}^{+500}$	3

present value corresponds to an  $\alpha$ -decay hindrance factor of  $\approx 1.1$ , which is typical for an  $\alpha$  decay proceeding between two states of identical spin and parity, hence removing the issue of anomalously large reduced  $\alpha$ -decay widths reported earlier.

#### IV. SUMMARY

The observations concerning the  $^{13/2^+} [\pi(i_{13/2})]$  state in  $^{201}\text{Fr}$  have been remarkably improved in this study. A level energy and a half-life of 289.5(4) keV and 720(40) ns were measured, respectively, corresponding to a  $B(M2)$  value of 0.17(2) W.u. Evidence for the  $M2$  character of the transition depopulating the state was provided. The present results of the  $^{13/2^+}$  isomeric state are in good agreement with those proposed in Ref. [13], as well as with the systematic pattern set by the observations of the same state in nearby nuclei. A systematic comparison of the  $^{13/2^+}$  level energy to the

ground-state deformation revealed a clear correlation between the two in the odd- $Z$  nuclei beyond lead.

#### ACKNOWLEDGMENTS

This work was supported by the Academy of Finland under Contracts No. 213503 (Finnish Center of Excellence Programme) and No. 323710 (Personal research project, K.A.). The authors also thank the GAMMAPOOL European Spectroscopy Resource for the loan of the germanium detectors. The contribution of A.H. was supported by the Slovak Research and Development Agency (Contract No. APVV-15-0225), the Slovak grant agency VEGA (Contract No. 2/0129/17), and the project ITMS code 26210120023, supported by the Research and Development Operational Programme funded by ERDF (30%).

- 
- [1] G. D. Dracoulis, P. M. Walker, and F. G. Kondev, *Rep. Prog. Phys.* **79**, 076301 (2016).
- [2] A. N. Andreyev, D. Ackermann, F. P. Heßberger, K. Heyde, S. Hofmann, M. Huyse, D. Karlgren, I. Kojouharov, B. Kindler, B. Lommel, G. Münzenberg, R. D. Page, K. Van de Vel, P. Van Duppen, W. B. Walters, and R. Wyss, *Phys. Rev. C* **69**, 054308 (2004).
- [3] E. Coenen, K. Deneffe, M. Huyse, P. Van Duppen, and J. L. Wood, *Z. Phys. A* **324**, 485 (1986).
- [4] H. Kettunen, T. Enqvist, T. Grahn, P. Greenlees, P. Jones, R. Julin, S. Juutinen, A. Keenan, P. Kuusiniemi, M. Leino, A.-P. Leppänen, P. Nieminen, J. Pakarinen, P. Rakhkila, and J. Uusitalo, *Eur. Phys. J. A* **17**, 537 (2003).
- [5] H. Kettunen, T. Enqvist, M. Leino, K. Eskola, P. Greenlees, K. Helariutta, P. Jones, R. Julin, S. Juutinen, H. Kankaanpää, H. Koivisto, P. Kuusiniemi, M. Muikku, P. Nieminen, P. Rakhkila, and J. Uusitalo, *Eur. Phys. J. A* **16**, 457 (2003).
- [6] K. Auranen, J. Uusitalo, S. Juutinen, U. Jakobsson, T. Grahn, P. T. Greenlees, K. Hauschild, A. Herzáň, R. Julin, J. Konki, M. Leino, J. Pakarinen, J. Partanen, P. Peura, P. Rakhkila, P. Ruotsalainen, M. Sandzelius, J. Sarén, C. Scholey, J. Sorri, and S. Stolze, *Phys. Rev. C* **90**, 024310 (2014).
- [7] K. Auranen, J. Uusitalo, S. Juutinen, H. Badran, F. D. Bisso, D. Cox, T. Grahn, P. T. Greenlees, A. Herzáň, U. Jakobsson *et al.*, *Phys. Rev. C* **95**, 044311 (2017).
- [8] J. Uusitalo, M. Leino, T. Enqvist, K. Eskola, T. Grahn, P. T. Greenlees, P. Jones, R. Julin, S. Juutinen, A. Keenan, H. Kettunen, H. Koivisto, P. Kuusiniemi, A.-P. Leppänen, P. Nieminen, J. Pakarinen, P. Rakhkila, and C. Scholey, *Phys. Rev. C* **71**, 024306 (2005).
- [9] U. Jakobsson, S. Juutinen, J. Uusitalo, M. Leino, K. Auranen, T. Enqvist, P. T. Greenlees, K. Hauschild, P. Jones, R. Julin, S. Ketelhut, P. Kuusiniemi, M. Nyman, P. Peura, P. Rakhkila, P. Ruotsalainen, J. Sarén, C. Scholey, and J. Sorri, *Phys. Rev. C* **87**, 054320 (2013).
- [10] U. Jakobsson, J. Uusitalo, S. Juutinen, M. Leino, T. Enqvist, P. T. Greenlees, K. Hauschild, P. Jones, R. Julin, S. Ketelhut, P. Kuusiniemi, M. Nyman, P. Peura, P. Rakhkila, P. Ruotsalainen, J. Sarén, C. Scholey, and J. Sorri, *Phys. Rev. C* **85**, 014309 (2012).
- [11] J. Uusitalo, J. Sarén, S. Juutinen, M. Leino, S. Eeckhaudt, T. Grahn, P. T. Greenlees, U. Jakobsson, P. Jones, R. Julin, S. Ketelhut, A.-P. Leppänen, M. Nyman, J. Pakarinen, P. Rakhkila, C. Scholey, A. Semchenkov, J. Sorri, A. Steer, and M. Venhart, *Phys. Rev. C* **87**, 064304 (2013).
- [12] Z. Kalaninová, A. N. Andreyev, S. Antalic, F. P. Heßberger, D. Ackermann, B. Andel, M. C. Drummond, S. Hofmann, M. Huyse, B. Kindler, J. F. W. Lane, V. Liberati, B. Lommel, R. D. Page, E. Rapisarda, K. Sandhu, S. Šáro, A. Thornthwaite, and P. Van Duppen, *Phys. Rev. C* **87**, 044335 (2013).
- [13] Z. Kalaninová, S. Antalic, A. N. Andreyev, F. P. Heßberger, D. Ackermann, B. Andel, L. Bianco, S. Hofmann, M. Huyse, B. Kindler, B. Lommel, R. Mann, R. D. Page, P. J. Sapple, J. Thomson, P. Van Duppen, and M. Venhart, *Phys. Rev. C* **89**, 054312 (2014).
- [14] P. Nieminen, S. Juutinen, A. N. Andreyev, J. F. C. Cocks, O. Dorvaux, K. Eskola, P. T. Greenlees, K. Hauschild, K. Helariutta, M. Huyse *et al.*, *Phys. Rev. C* **69**, 064326 (2004).
- [15] K. Auranen, J. Uusitalo, S. Juutinen, U. Jakobsson, T. Grahn, P. T. Greenlees, K. Hauschild, A. Herzáň, R. Julin, J. Konki *et al.*, *Phys. Rev. C* **91**, 024324 (2015).
- [16] K. Auranen, J. Uusitalo, S. Juutinen, H. Badran, F. Defranchi Bisso, D. Cox, T. Grahn, P. T. Greenlees, A. Herzáň, U. Jakobsson *et al.*, *Phys. Rev. C* **97**, 024301 (2018).
- [17] U. Jakobsson, J. Uusitalo, S. Juutinen, M. Leino, P. Nieminen, K. Andgren, B. Cederwall, P. T. Greenlees, B. Hadinia, P. Jones *et al.*, *Phys. Rev. C* **82**, 044302 (2010).
- [18] M. Nyman, S. Juutinen, I. Darby, S. Eeckhaudt, T. Grahn, P. T. Greenlees, U. Jakobsson, P. Jones, R. Julin, S. Ketelhut, H. Kettunen, M. Leino, P. Nieminen, P. Peura, P. Rakhkila, J. Sarén, C. Scholey, J. Sorri, J. Uusitalo, and T. Enqvist, *Phys. Rev. C* **88**, 054320 (2013).
- [19] M. Leino, J. Äystö, T. Enqvist, P. Heikkinen, A. Jokinen, M. Nurmi, A. Ostrowski, W. Trzaska, J. Uusitalo, K. Eskola, P. Armbruster, and V. Ninov, *Nucl. Instrum. Methods Phys. Res., Sect. B* **99**, 653 (1995).
- [20] J. Sarén, J. Uusitalo, M. Leino, and J. Sorri, *Nucl. Instrum. Methods Phys. Res., Sect. A* **654**, 508 (2011).
- [21] R. Page, A. Andreyev, D. Appelbe, P. Butler, S. Freeman, P. Greenlees, R.-D. Herzberg, D. Jenkins, G. Jones, P. Jones, D. Joss, R. Julin, H. Kettunen, M. Leino, P. Rakhkila, P. Regan, J. Simpson, J. Uusitalo, S. Vincent, and R. Wadsworth, *Nucl. Instrum. Methods Phys. Res., Sect. B* **204**, 634 (2003).

- [22] P. Rakhila, *Nucl. Instrum. Methods Phys. Res., Sect. A* **595**, 637 (2008).
- [23] K. Schmidt, *Eur. Phys. J. A* **8**, 141 (2000).
- [24] T. Kibédi, T. W. Burrows, M. B. Trzhaskovskaya, P. M. Davidson, and C. W. Nesotr, Jr., *Nucl. Instrum. Methods Phys. Res., Sect. A* **589**, 202 (2008).
- [25] A. Hürstel, Y. Le Coz, E. Bouchez, A. Chatillon, A. Görgen, P. T. Greenlees, K. Hauschild, S. Juutinen, H. Kettunen, W. Korten *et al.*, *Eur. Phys. J. A* **21**, 365 (2004).
- [26] A. Herzán, S. Juutinen, K. Auranen, T. Grahn, P. T. Greenlees, K. Hauschild, U. Jakobsson, P. Jones, R. Julin, S. Ketelhut *et al.*, *Phys. Rev. C* **92**, 044310 (2015).
- [27] A. Herzán, S. Juutinen, K. Auranen, T. Grahn, P. T. Greenlees, K. Hauschild, U. Jakobsson, R. Julin, S. Ketelhut, M. Leino *et al.*, *Phys. Rev. C* **96**, 014301 (2017).
- [28] G. K. Mabala, E. Gueorguieva, J. F. Sharpey-Schafer, M. Benatar, R. W. Fearick, K. I. Korir, J. J. Lawrie, S. M. Mullins, S. H. T. Murray, N. J. Ncapayi, R. T. Newman, D. G. Roux, F. D. Smit, and R. Wyss, *Eur. Phys. J. A* **25**, 49 (2005).
- [29] W. F. Piel, T. Chapuran, K. Dybdal, D. B. Fossan, T. Lönnroth, D. Horn, and E. K. Warburton, *Phys. Rev. C* **31**, 2087 (1985).
- [30] T. Lönnroth, *Z. Phys. A: Atoms Nuclei* **307**, 175 (1982).
- [31] T. Lönnroth and B. Fant, *Phys. Scr.* **18**, 172 (1978).
- [32] A. Hürstel, M. Rejmund, E. Bouchez, P. Greenlees, K. Hauschild, S. Juutinen, H. Kettunen, W. Korten, Y. Le Coz, P. Nieminen *et al.*, *Eur. Phys. J. A: Hadrons Nuclei* **15**, 329 (2002).
- [33] K. Andgren, U. Jakobsson, B. Cederwall, J. Uusitalo, T. Bäck, S. J. Freeman, P. T. Greenlees, B. Hadinia, A. Hugues, A. Johnson *et al.*, *Phys. Rev. C* **78**, 044328 (2008).
- [34] R. Davie, A. Poletti, G. Dracoulis, A. Byrne, and C. Fahlander, *Nucl. Phys. A* **430**, 454 (1984).
- [35] S. Bayer, A. Byrne, G. Dracoulis, A. Baxter, T. Kibédi, and F. Kondev, *Nucl. Phys. A* **694**, 3 (2001).
- [36] S. Hilaire and M. Girod, *Eur. Phys. J. A* **33**, 237 (2007).
- [37] P. Möller, A. J. Sierk, T. Ichikawa, and H. Sagawa, *At. Data Nucl. Data Tables* **109-110**, 1 (2016).
- [38] M. R. Pearson, P. Campbell, K. Leerunnavarat, J. Billowes, I. S. Grant, M. Keim, J. Kilgallon, I. D. Moore, R. Neugart, M. Neuroth, S. Wilbert, and the ISOLDE Collaboration, *J. Phys. G: Nucl. Part. Phys.* **26**, 1829 (2000).
- [39] A. E. Barzakh, D. V. Fedorov, V. S. Ivanov, P. L. Molkanov, F. V. Moroz, S. Y. Orlov, V. N. Panteleev, M. D. Seliverstov, and Y. M. Volkov, *Phys. Rev. C* **94**, 024334 (2016).
- [40] A. E. Barzakh, D. V. Fedorov, V. S. Ivanov, P. L. Molkanov, F. V. Moroz, S. Y. Orlov, V. N. Panteleev, M. D. Seliverstov, and Y. M. Volkov, *Phys. Rev. C* **95**, 044324 (2017).
- [41] J. G. Cubiss, A. E. Barzakh, M. D. Seliverstov, A. N. Andreyev, B. Andel, S. Antalic, P. Ascher, D. Atanasov, D. Beck, J. Bieroń *et al.*, *Phys. Rev. C* **97**, 054327 (2018).
- [42] K. M. Lynch, J. Billowes, M. L. Bissell, I. Budinčević, T. E. Cocolios, R. P. De Groote, S. De Schepper, V. N. Fedosseev, K. T. Flanagan, S. Franchoo, R. F. Garcia Ruiz, H. Heylen, B. A. Marsh, G. Neyens, T. J. Procter, R. E. Rossel, S. Rothe, I. Strashnov, H. H. Stroke, and K. D. A. Wendt, *Phys. Rev. X* **4**, 011055 (2014).
- [43] J. O. Rasmussen, *Phys. Rev.* **113**, 1593 (1959).